

Photoresponsive Coumarin-Stabilized Polymeric Nanoparticles as a Detectable Drug Carrier

Jae Woo Chung, KangAe Lee, Colin Neikirk, Celeste M. Nelson, and Rodney D. Priestley*

The ability to create aqueous suspended stable nanoparticles of the hydrophobic homopolymer poly(ϵ -caprolactone) end-functionalized with coumarin moieties (CPCL) is demonstrated. Nanoparticles of CPCL are prepared in a continuous manner using nanoprecipitation. The resulting nanoparticles are spherical in morphology, about 40 nm in diameter, and possess a narrow size distribution and excellent stability over 4 months by repulsive surface charge. Nanoparticle size can be easily controlled by manipulating the concentration of CPCL in the solution. The interparticle assembly between the nanoparticles can be reversibly adjusted with photoirradiation due to photoinduced [2 + 2] cyclodimerization and cleavage between the coumarin molecules. In addition, the CPCL nanoparticles show significant cellular uptake without cytotoxicity, and the intrinsic fluorescence of the coumarin functional group permits the direct detection of cellular internalization.

1. Introduction

Over the past few decades polymeric nanoparticles have attracted significant attention due to their promise in applications for drug transportation and medical imaging.^[1] Generally, for the formation of stable polymeric nanoparticles in an aqueous medium, most nanoparticles have been designed with an amphiphilic core/shell structure, that is, a hydrophobic inner core and a hydrophilic outer shell, using amphiphilic block copolymers.^[1c] Such polymeric nanoparticles can readily incorporate hydrophobic drugs into their cores, and the hydrophilic shell can stabilize the hydrophobic core in water. However, this approach typically requires that the block copolymers are prepared via controlled living

polymerization, a more complex synthetic method relative to conventional polymerization.^[2] At the minimum, approaches to stabilize nanoparticles that mitigate the use of block copolymers may prove more facile in particle preparation and more cost-effective. Conversely, the potential benefits of stimuli-responsive nanoparticles, which respond to changes based on their environment or an external stimulus, in controlled drug delivery, such as triggered payload release, provide an incentive for the continued development of such types of nanoparticles.^[3]

Of growing interest are polymeric nanoparticles containing coumarin moieties because they are both responsive, via the reversible photoresponsive [2 + 2] cyclodimerization,^[4] and exhibit intrinsic fluorescence.^[5] This makes them tremendously attractive in applications ranging from size-tunable systems involving photoinduced crosslinking and cleavage between coumarin molecules to the marker for the detectable delivery of hydrophobic drugs.^[2,6,7] Yet, the use of coumarin molecules in the formulation of nanoparticles has been limited to approaches utilizing amphiphilic block copolymers.

Herein, we demonstrate reversibly photoresponsive coumarin-stabilized polymeric nanoparticles in an aqueous medium, which act as a detectable drug carrier without the usage of an amphiphilic structure and additional fluorescent probes. The nanoparticles are spherical in morphology with diameter about 40 nm, and possess a narrow size distribution

Dr. J. W. Chung, Dr. K. Lee, C. Neikirk,
Prof. C. M. Nelson, Prof. R. D. Priestley
Department of Chemical and Biological Engineering
Princeton University
Princeton, NJ 08544, USA
E-mail: rpriestl@princeton.edu
Dr. K. Lee, Prof. C. M. Nelson
Department of Molecular Biology
Princeton University
Princeton, NJ 08544, USA



DOI: 10.1002/sml.201102263

and excellent stability, although they are composed of a hydrophobic homopolymer. The interparticle assembly between the nanoparticles can be reversibly adjusted by photocrosslinking and cleavage of the coumarin molecules exposed at the nanoparticle surface. In addition, the nanoparticles exhibit an enhanced rate of cellular uptake without significant cytotoxicity, and the intrinsic fluorescence of the coumarin functional group permits the detection of cellular internalization.

2. Experimental Section

2.1. Materials

Polycaprolactone diol (PCL-diol, $M_n = 2000$), ethyl bromoacetate (98%), potassium acetate ($\geq 99\%$), hydrochloric acid (36.8%), thionyl chloride, and triethylamine (TEA, $\geq 99\%$) were purchased from Sigma–Aldrich Chemical Company. 7-Hydroxycoumarin (99%), 1,4-dioxane (99.5%), and tetrahydrofuran (THF, HPLC) were purchased from Acros Organics. Acetone (HPLC), ethanol (anhydrous), methanol (99.5%), and sodium hydroxide were supplied by Fisher Scientific. The deionized water used in this study had a resistance above 18.0 M Ω .

2.2. Preparation of Polymeric Nanoparticles

As shown in **Figure 1**, the coumarin derivative, 7-chlorocarbonylmethoxycoumarin, was first synthesized from 7-hydroxycoumarin and subsequently reacted with the hydroxyl ends of PCL ($M_n = 2000$ g mol $^{-1}$) via acylation, which resulted in coumarin end-functionalized PCL (CPCL, $M_n = 2700$ g mol $^{-1}$).^[4d] **Figure 2** schematically illustrates the nanoparticle preparation procedure. Briefly, the CPCL nanoparticles were produced by a flash nanoprecipitation method using a confined impinging jet mixer composed of two separate streams: CPCL/THF solution and water.^[8] THF was removed from the resulting mixture to obtain CPCL nanoparticles suspended in water. Detailed experimental procedures and synthesis results are reported in the Supporting Information. The resulting CPCL nanoparticles were denoted as CPCL $_x$ (where x represents the amount (mg) of CPCL dissolved in THF).

2.3. Photoirradiation

Photodimerization and cleavage of coumarin moieties in CPCL nanoparticles were accomplished using a UVGL-58 handheld UV lamps (6 W) at $\lambda = 365$ and 254 nm, respectively. UV irradiation of the aqueous CPCL nanoparticle solution was carried out in a quartz cuvette with a 1 cm optical length and the distance between the cuvette and lamp was kept at 1 cm during the measurements.

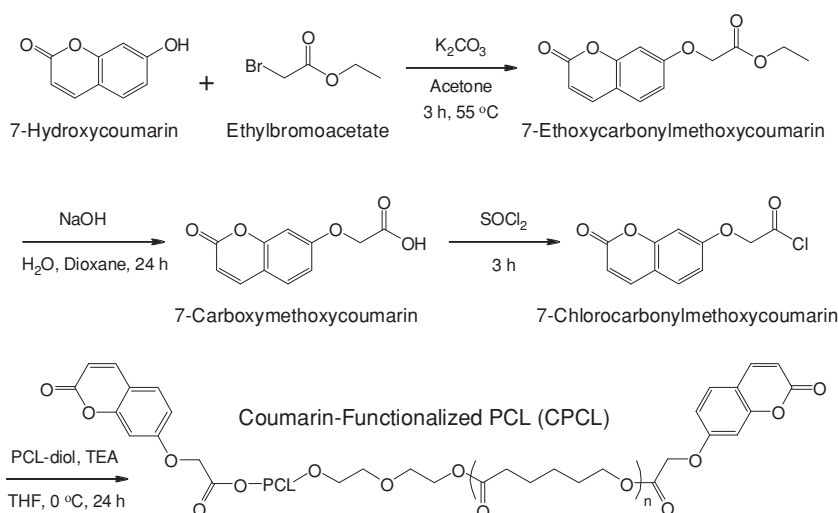


Figure 1. Synthetic scheme for coumarin-functionalized PCL (CPCL).

2.4. Characterization

The ^1H nuclear magnetic resonance (^1H NMR) spectra were recorded in either $[\text{D}_6]\text{DMSO}$ or CDCl_3 on a Bruker Avance-II 500 MHz spectrometer to verify the synthesis of coumarin derivatives and CPCL. Size exclusion chromatography (SEC) was performed on a system equipped with a Waters 515 solvent pump, a Waters 717 autosampler, and a Waters 410 differential refractometer that had been modified with a Precision Detectors PD2020 light scattering detector operating at 680 nm. The SEC utilized a Viscotek I-series guard column connected in series with a Viscotek low-molecular-weight I-series column, and a Viscotek mid-molecular-weight I-series column. A mobile phase comprising dimethylformamide (DMF) with 0.02 M ammonium acetate that had been filtered through 0.2 μm filters was used. A flow rate of 1 mL min $^{-1}$ was employed with the columns and detectors set at 40 °C. Differential scanning calorimetry (DSC) analysis was performed using a TA DSC Q2000 apparatus under N_2 flow. All of the samples were first heated from -90 to 130 °C at 20 °C min $^{-1}$ to erase the thermal history, then

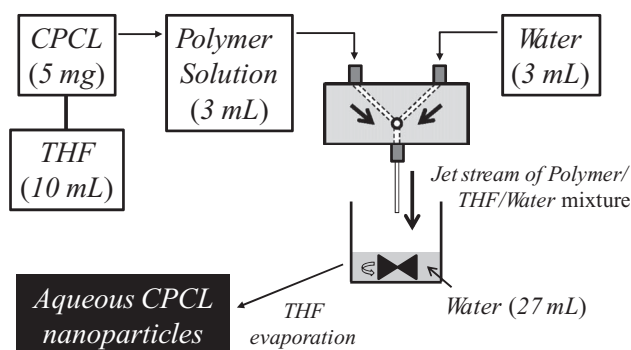


Figure 2. Schematic illustration of the preparation of aqueous suspended CPCL nanoparticles using the flash nanoprecipitation method.

cooled to $-90\text{ }^{\circ}\text{C}$ at $20\text{ }^{\circ}\text{C min}^{-1}$, and finally heated to $130\text{ }^{\circ}\text{C}$ at $20\text{ }^{\circ}\text{C min}^{-1}$. The morphology of PCL and CPCL nanoparticles was visualized by field-emission scanning electron microscopy (FE-SEM, XL30 FEG-SEM). The FE-SEM samples were coated with a thin conductive Ir layer (thickness: 5 nm) prior to observation. Transmission electron microscopy (TEM) images (Philips CM100 TEM, 100 keV) were taken of the direct sampling of the CPCL solution on carbon-coated copper grids. Diameters and size distributions of the nanoparticles suspended in water were determined using dynamic light scattering (DLS; Malvern Instruments Zetasizer Nano-ZS ZEN 3600). Measurements were performed at a 173° angle for 3 min and repeated a minimum of three times per sample. The measured time correlation functions were analyzed by autocorrelation using the method of the cumulants, thereby providing an average value of the intensity-average particle size and particle polydispersity index (PDI). Intensity-average and number-average particle size distributions were calculated using the Laplace inversion program, CONTIN. Zeta potentials of nanoparticle samples were also obtained using the same instrument (Malvern Instruments Zetasizer Nano-ZS ZEN 3600). The instrument performed laser Doppler velocimetry to obtain the electrophoretic mobility, which was then converted to a zeta potential via the Smoluchowski equation. The progress of dimerization and cleavage of coumarin moieties in CPCL nanoparticles by photoirradiation at $\lambda = 365$ and 254 nm , respectively, was followed by UV/Vis absorption spectrometry (Agilent UV-Visible ChemStation, Model 8453) in the range of 200–800 nm with 1 nm resolution. A quartz cuvette with a 1 cm optical length was used and the aqueous CPCL nanoparticle solution was directly used for UV/Vis measurements without any treatment.

2.5. Cell Culture and Cellular Uptake Test

Human embryonic kidney (HEK) 293 cells were maintained in growth medium comprising Dulbecco's modified Eagle's medium (DMEM, Hyclone) supplemented with 10% heat-inactivated fetal bovine serum (Atlanta Biologicals) and gentamicin ($50\text{ }\mu\text{g mL}^{-1}$, Sigma). Cells were grown at $37\text{ }^{\circ}\text{C}$ with 5% CO_2 in a humidified incubator. For qualitative cellular uptake analysis of CPCL nanoparticles, HEK 293 cells were treated with CPCL ($30\text{ }\mu\text{g mL}^{-1}$) nanoparticles and incubated for 24 h. After incubation, excess particles were removed and the cells were washed three times with cold phosphate-buffered saline (PBS), and then fixed with 4% formaldehyde in PBS. Cellular uptake of CPCL nanoparticles was visualized at $\lambda_{\text{ex}} = 360\text{ nm}$ and $\lambda_{\text{em}} = 450\text{ nm}$ using a Hamamatsu Orca CCD camera attached to a Nikon Eclipse Ti microscope. For quantitative cellular uptake analysis, HEK 293 cells were incubated with a range of concentrations from 0 to $30\text{ }\mu\text{g mL}^{-1}$ for 24 h, washed three times with cold PBS, and lysed with lysis buffer (25 mM glycylglycine (pH 7.8), 15 mM MgSO_4 , 4 mM ethylene glycol tetraacetic acid, 1% Triton X-100, and 1 mM dithiothreitol). Cellular debris was removed by centrifugation at 13 000 rpm for 10 min. Supernatant was transferred into 96-well optiplates and fluorescence intensity was determined using a GloMax-Multi Detection

System (Promega Co.) with $\lambda_{\text{ex}} = 360\text{ nm}$ and $\lambda_{\text{em}} = 450\text{ nm}$. Experiments were performed three times independently.

2.6. Cellular Cytotoxicity

Cell viability was determined using the 3-(4,5-dimethylthiazol-2-yl)-5-(3-carboxymethoxyphenyl)-2-(4-sulfophenyl)-2H-tetrazolium (MTS, Promega Co.) assay. HEK 293 cells were incubated with CPCL nanoparticles with a range of concentrations from 0 to $120\text{ }\mu\text{g mL}^{-1}$ for 48 h. MTS solution was added for 2 h. The absorbance was measured at 490 nm using a GloMax-Multi Detection System (Promega Co.). Experiments were performed three times independently.

3. Results and Discussion

Figure 3a and b shows morphological images of CPCL5 nanoparticles visualized by FE-SEM and TEM, respectively. The CPCL5 nanoparticles were spherical in morphology and

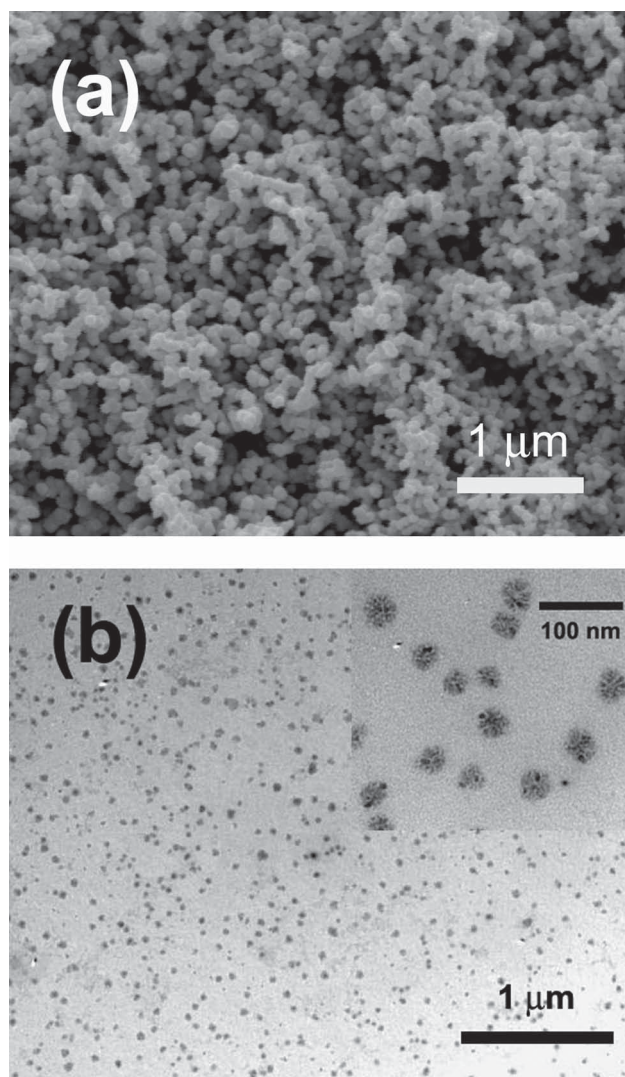


Figure 3. Morphology of CPCL5 nanoparticles visualized by a) FE-SEM and b) TEM.

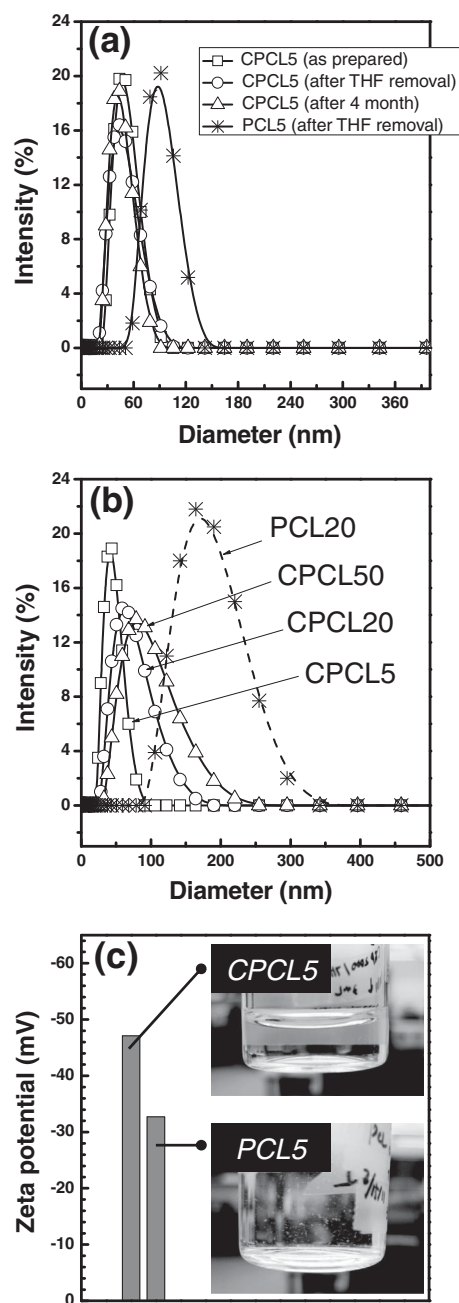


Figure 4. a) DLS plots of CPCL5 and PCL5. b) DLS plots of size-controlled nanoparticles (CPCL5, 20, 50) achieved by manipulating the concentration of CPCL in THF. c) Zeta-potential graph of CPCL5 and PCL5; inset images: CPCL5 and PCL5 nanoparticle aqueous solutions 4 months after nanoparticle preparation.

possessed a narrow size distribution. In particular, TEM revealed that the CPCL5 nanoparticles about 40 nm in diameter were well dispersed and isolated in an aqueous medium. To further evaluate the size of the nanoparticles, DLS measurements were carried out. The DLS results (**Figure 4a**) clearly showed that much smaller nanoparticles could be produced from CPCL5 (Z-average diameter =

40.8 nm) compared to PCL5 (Z-average diameter = 101.7 nm), which does not contain coumarin moieties; this was consistent with the TEM results. In addition, there was no change in the size of CPCL5 nanoparticles after THF removal, and the sizes were stable over 4 months. The nanoparticle size could also be easily controlled by manipulating the concentration of CPCL in the THF solution. The size of CPCL nanoparticles increased with increasing amount of CPCL, as shown in **Figure 4b**. CPCL20 also showed a smaller size than PCL20. Detailed size information for the nanoparticles is summarized in **Table 1**.

To form stable polymeric nanoparticles in an aqueous medium, most approaches rely on the design of polymeric nanoparticles with an amphiphilic core/shell structure.^[1c] Interestingly, the CPCL nanoparticles were small and well dispersed with narrow size distribution and excellent stability in water, despite the fact that they lacked a hydrophilic outer shell and did not contain any additive surfactants. The results strongly suggest that the coumarin functionality at the end of each PCL chain played an important role in the formation and stability of the nanoparticles. To investigate the effect of coumarin molecules on nanoparticle formation, we measured the zeta potential of CPCL5 and PCL5. As shown in **Figure 4c**, the CPCL5 nanoparticles (−47.1 mV) exhibited a more negative surface charge than the PCL nanoparticles (−32.7 mV). In addition, there was no evidence of agglomeration for CPCL5 nanoparticles in water after 4 months, whereas agglomeration occurred for PCL5 nanoparticles after 72 h. This result indicates the good stability of CPCL5 nanoparticles (see inset images in **Figure 4c**). It should be noted that gold nanoparticles protected by citrate molecules show good stability in aqueous medium due to repulsive forces caused by a strong negative surface charge of approximately −43 mV.^[9] Based on zeta-potential measurements, we suggest that the smaller size and increased stability of CPCL5 compared to PCL5 nanoparticles can be attributed to the repulsion caused by strong negative surface charges on the nanoparticles due to the introduction of coumarin moieties.

It is well known that the photoirradiation ($\lambda > 300$ nm) of coumarin results in photochemical dimerization between coumarin molecules by [2 + 2] cyclobutane ring formation, and that the cyclobutane rings can be photocleaved upon irradiation with light of shorter wavelength ($\lambda < 260$ nm).^[4] Zhao et al. reported amphiphilic block copolymer micelles with coumarin pendants for the stabilization of micelles by UV-induced crosslinking.^[7] Jiang and co-workers also studied the stabilization and morphology switching of the polymer vesicles using coumarin molecules.^[6] As mentioned above, most

Table 1. Sizes of PCL and CPCL nanoparticles as measured by DLS.

Samples	Diameter at mean intensity [nm]	Z-Average diameter [nm]	Width [nm]	PDI
PCL5	108.4	101.7	28.4	0.051
PCL20	191.6	169.8	71.5	0.123
CPCL5	43.9	40.8	11.6	0.061
CPCL20	68.3	60.1	26.0	0.131
CPCL50	88.9	76.7	35.8	0.136

research on coumarin molecules in the nanoparticle literature has focused on the stabilization of nanoparticles for controlled drug release using photoreversible coumarin dimerization, but there are no studies on the effect of coumarin on nanoparticle formation and stability in aqueous medium. To the best of our knowledge, this is the first report to illustrate that coumarin moieties can lead to stable polymeric nanoparticle formation in an aqueous medium, although the reason that coumarin moieties provide negative charge stability to the nanoparticles is not fully understood.

Recently, increasing attention has been paid to photocrosslinkable polymer nanoparticles (or colloids) on account of their environmental and biomedical usage. Akashi et al. reported the reversible size change of the nanoparticles by photodimerization and cleavage of cinnamate groups in the polymer backbone.^[10] Zillessen et al. reported polystyrene colloids capable of cluster formation via photochemical crosslinking of benzophenone in the polystyrene side chain.^[11] However, these nanoparticles were unstable in water or showed irreversible photocrosslinking. Although Schärfl et al. reported cinnamate- or coumarin-labeled

poly(organosiloxane) nanoparticles capable of photoreversible cluster formation, the nanoparticles were still dispersed in THF or toluene.^[12] On the other hand, the CPCL nanoparticles studied herein were not only stable in water but also composed of a biodegradable polymer, approved by the FDA for use in biomedical applications, and reversibly photocrosslinkable coumarin moieties.

Thus, we investigated the effect of photoirradiation on the CPCL nanoparticles in aqueous medium using UV/Vis and DLS analysis. As expected, UV/Vis absorbance at 320 nm, which corresponds to the characteristic absorbance of the double bond in the benzopyrone ring of coumarin,^[13] decreased upon photoirradiation at $\lambda = 365$ nm, thus indicating the photodimerization of coumarins in CPCL5 nanoparticles (see **Figure 5a**). Furthermore, the UV/Vis absorbance at 320 nm increased upon photoirradiation at $\lambda = 254$ nm, as shown in the inset plots of Figure 5a, which indicates the photocleavage of dimerized coumarin moieties. Figure 5b clearly shows the photoreversibility of CPCL nanoparticles in water when exposed to a suitable wavelength of UV light. The photodimerization/photocleavage (365/254 nm irradiation)

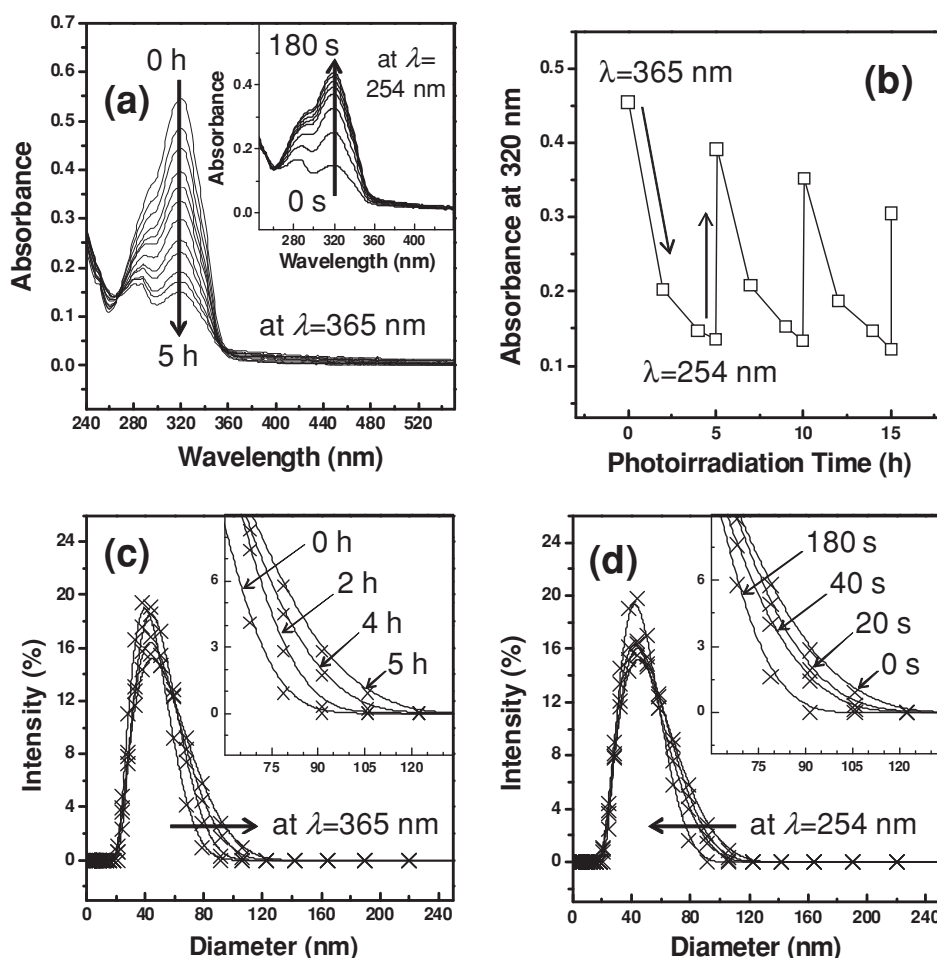


Figure 5. a) UV/Vis plots of aqueous CPCL5 nanoparticles upon photoirradiation at $\lambda = 365$ nm as a function of time for 5 h (inset: UV/Vis plots of aqueous CPCL5 nanoparticles upon photoirradiation at $\lambda = 254$ nm as a function of time after photoirradiation at $\lambda = 365$ nm for 5 h). b) Absorbance changes of CPCL nanoparticles at 320 nm upon alternate irradiation with 365 and 254 nm UV light. c) DLS plots of CPCL5 nanoparticles with photoirradiation at $\lambda = 365$ nm as a function of time. d) DLS plots of CPCL5 nanoparticles with photoirradiation at $\lambda = 254$ nm as a function of time after photoirradiation at $\lambda = 365$ nm for 5 h.

cycle was repeated three times. The photocrosslinking reaction appears much slower than the reverse photoscission reaction. The highest absorbance change for the coumarin dimerization in CPCL nanoparticles was achieved after 5 h of irradiation at 365 nm. The reverse reaction, that is, photocleavage of dimerized coumarin molecules in CPCL nanoparticles, was allowed to proceed for only 180 s. However, the absorption intensity did not completely recover to the original level after photoirradiation at $\lambda = 254$ nm, which indicates that some of the coumarin dimer in the CPCL nanoparticles did not revert back to the starting material. In particular, the recovery efficiency decreased with each repetition of the photodimerization/photocleavage cycle. This phenomenon has been found to be the result of a dynamic equilibrium, with crosslinking and scission occurring at 254 nm.^[14]

The reversible photoresponsive behavior of coumarin moieties in the CPCL5 nanoparticles affected the size of the nanoparticles. As shown in Figure 5c, the size of the nanoparticles slightly increased with the degree of photodimerization of coumarins by irradiation at $\lambda = 365$ nm. On the other hand, photoirradiation at $\lambda = 254$ nm resulted in recovery to the original size of the nanoparticles by the photocleavage of the dimerized coumarin moieties (see Figure 5d). The change in size of the nanoparticles may be attributed to interparticle crosslinking and de-crosslinking, according to the schematic illustration proposed in Figure 6. Some particles combined together to form larger particles comprising two or three pristine particles due to photodimerization between coumarin units on the surface of the nanoparticles. A large change in size was not observed upon photoirradiation, as reported by Jiang and co-workers,^[2] because coumarin moieties are mostly present in the interior of the nanoparticle due to its hydrophobicity.^[6] In addition, the repulsive interactions of the CPCL nanoparticles are likely to hinder the nanoparticles from approaching close enough to form

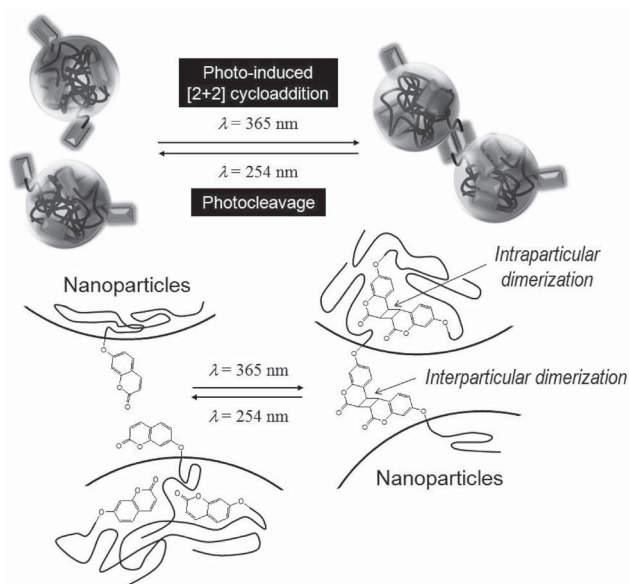


Figure 6. Schematic illustration of the photoresponsive behavior of CPCL nanoparticles by photoinduced [2 + 2] cycloaddition and cleavage of coumarin moieties in the nanoparticles.

interparticle crosslinks.^[11] Nevertheless, the current approach demonstrated the potential interest of a new concept that consists in using light to assemble hydrophobic nanoparticles through photocrosslinking. More studies are under way in our laboratory to understand the effect of coumarin molecules on the polymeric nanoparticle formation and to enhance the efficiency of the particular assembly.

Generally, the therapeutic effects of drug carriers depend on their cellular uptake, and systems to detect nanoparticle internalization would be ideal for monitoring drug pharmacokinetics. Coumarin is a fluorescent marker which has proven useful for incorporation into nanoparticles due to its biocompatibility, high fluorescence activity, low dye loading, and low rate of leakiness.^[5] Thus, end functionalization of PCL with coumarin not only increases the stability of the nanoparticles but also enables the detection of their intracellular internalization. Fluorescence of CPCL nanoparticles was detected at an excitation wavelength of 360 nm and increased in a dose-dependent manner (Figure 7a). Cellular uptake of CPCL nanoparticles was visualized in human embryonic kidney (HEK) 293 cells (Figure 7b). CPCL nanoparticles were detected primarily around the periphery of the nuclear membrane and throughout the cytoplasm, which is consistent with previous findings of subcellular localization of PCL nanoparticles.^[15] CPCL also aggregated at the cell membrane, thus suggesting the possibility that CPCL may be internalized into cells through endocytosis and dispersed homogeneously into the cells.^[16] The fluorescence intensity of CPCL in cells increased as the CPCL concentration increased, with a plateau at $25 \mu\text{g mL}^{-1}$ (Figure 7c). Furthermore, as shown in Figure 7d, the viability of cells was not affected by uptake of CPCL nanoparticles, as determined using the MTS assay, suggesting minimal cytotoxicity. These results reveal that CPCL nanoparticles had an excellent cellular uptake property and can be potentially used as a detectable drug carrier. In particular, because the CPCL nanoparticles had a photoresponsive surface functionality capable of forming a photocrosslink due to the coumarin molecules, we anticipate further reversible surface functionalization of the nanoparticles using the coumarin molecules connected with specific target agents such as a stealth shell, cancer target, cell-penetrating agent, and imaging agent, thereby resulting in an advanced functional drug carrier with highly efficient drug delivery.

4. Conclusion

We have demonstrated that coumarin moieties that were end-functionalized to PCL, a biodegradable polymer, led to the formation of small polymeric nanoparticles with a narrow size distribution in an aqueous medium stabilized by strong negative surface charge. The size of the nanoparticles could be easily manipulated by controlling the polymer concentration. The CPCL nanoparticles showed slight reversible assembly upon photoirradiation and noncytotoxic cellular uptake. Moreover, the nanoparticles could be imaged within the cell due to the intrinsic fluorescence of coumarin. An advantage of our nanoparticles is that they were stabilized in an aqueous medium by coumarin, a bio-derived and

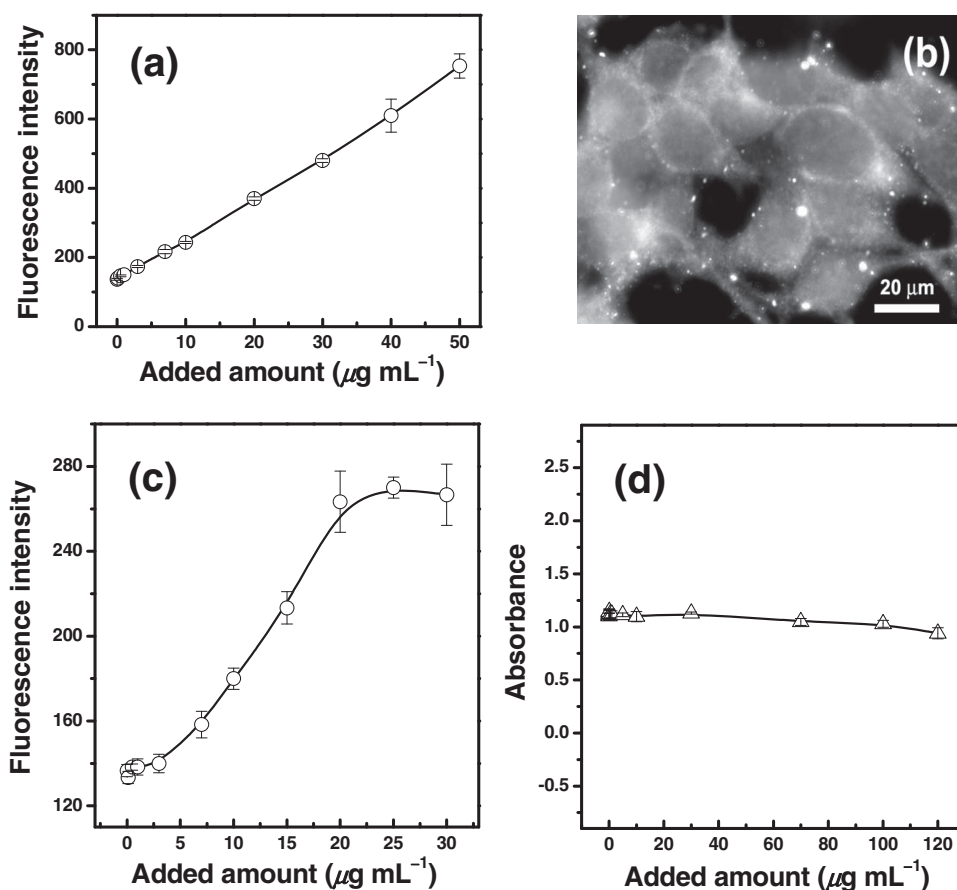


Figure 7. a) Dose-dependent increase in fluorescence intensity of CPCL nanoparticles at $\lambda_{\text{ex}} = 360$ nm and $\lambda_{\text{em}} = 450$ nm. b) Visualization of cellular internalization of CPCL nanoparticles. c) Dose-dependent increase in cellular uptake of CPCL nanoparticles. d) Cell viability and cytotoxicity determined by MTS assay.

-compatible molecule, without the additional usage of stabilizers. The simplicity of preparation and stimuli response of the coumarin-containing polymeric nanoparticles make them attractive for various potential applications as a tailor-made advanced functional drug carrier.

Supporting Information

Supporting Information is available from the Wiley Online Library or from the author.

Acknowledgements

We acknowledge usage of the PRISM Imaging and Analysis Center, which is supported in part by the NSF MRSEC program through the Princeton Center for Complex Materials (DMR-0819860). R.D.P. acknowledges the donors of the American Chemical Society Petroleum Research Fund for partial support of this work (PRF 49903-DNI10) and the 3M-nontenured faculty grant program for partial support of this work. C.M.N. acknowledges the NIH (GM083997 and HL110335), Susan G. Komen for the Cure (FAS0703855),

the David and Lucile Packard Foundation, and the Alfred P. Sloan Foundation for support of this work. We thank Professor L. Loo for the use of UV/Vis apparatus and Mr. Chuan Zhang for stimulating discussions during the preparation of this manuscript.

- [1] a) R. Gref, Y. Mianmitake, M. T. Peracchia, V. S. Trebetsky, V. P. Torchilin, R. Langer, *Science* **1994**, *263*, 1600–1603; b) K. Yasugi, Y. Nagasaki, M. Kato, K. Kataoka, *J. Controlled Release* **1999**, *62*, 89–100; c) G. S. Kwon, T. Okano, *Adv. Drug Delivery Rev.* **1996**, *21*, 107–116.
- [2] X. Jiang, R. Wang, Y. Ren, J. Yin, *Langmuir* **2009**, *25*, 9629–9632.
- [3] a) D. E. Owens III, Y. C. Jian, J. E. Fang, B. V. Slaughter, Y. H. Chen, N. A. Peppas, *Macromolecules* **2007**, *40*, 7306–7310; b) Y. F. Zhang, S. Z. Luo, S. Y. Liu, *Macromolecules* **2005**, *38*, 9813–9820; c) N. Hantzschel, F. B. Zang, F. Eckert, A. Pich, M. A. Winnik, *Langmuir* **2007**, *23*, 10793–10800; d) R. K. Reilly, C. J. Hawker, K. L. Wooley, *Chem. Soc. Rev.* **2006**, *35*, 1068–1083; e) C. Vancaeyzeele, V. Baranov, L. Shen, A. Abdelrahman, M. A. Winnik, *J. Am. Chem. Soc.* **2007**, *129*, 13653–13660; f) F. H. Meng, Z. Y. Zhong, J. Feijen, *Biomacromolecules* **2009**, *10*, 197–209.
- [4] a) G. S. Hammond, C. A. Stout, A. A. Lamola, *J. Am. Chem. Soc.* **1964**, *86*, 3103–3106; b) S. R. Trenor, A. R. Shultz, B. J. Love, T. E. Long, *Chem. Rev.* **2004**, *104*, 3059–3078; c) T. Matsuda, M. Mizutani, S. C. Arnold, *Macromolecules* **2000**, *33*, 795–800; d) S. R. Trenor, T. E. Long, B. J. Love, *Macromol. Chem. Phys.* **2004**, *205*, 715–723.

- [5] K. Y. Win, S.-S. Feng, *Biomaterials* **2005**, *26*, 2713–2722.
- [6] J. Jiang, Q. Shu, X. Chen, Y. Yang, C. Yi, X. Song, X. Liu, M. Chen, *Langmuir* **2010**, *26*, 14247–14254.
- [7] J. Jiang, B. Qi, M. Lepage, Y. Zhao, *Macromolecules* **2007**, *40*, 790–792.
- [8] C. Zhang, V. J. Pansare, R. K. Prud'homme, R. D. Priestley, *Soft Matter* **2012**, *8*, 86–93.
- [9] X. Lian, J. Jin, J. Tian, H. Zhao, *ACS Appl. Mater. Interfaces* **2010**, *2*, 2261–2268.
- [10] D. Shi, M. Matsusaki, T. Kaneko, M. Akashi, *Macromolecules* **2008**, *41*, 8167–8172.
- [11] A. Zillessen, E. Bartsch, *Langmuir* **2010**, *26*, 89–96.
- [12] X. Yuan, K. Fischer, W. Schärtl, *Adv. Funct. Mater.* **2004**, *14*, 457–463.
- [13] Q. Fu, L. Cheng, Y. Zhang, W. Shi, *Polymer* **2008**, *49*, 4981–4988.
- [14] M. Nagata, Y. Yamamoto, *React. Funct. Polym.* **2008**, *68*, 915–921.
- [15] L. Mei, Y. Zhang, Y. Zheng, G. Tian, C. Song, D. Yang, H. Chen, H. Sung, Y. Tian, Y. K. Liu, Z. Li, L. Huang, *Nanoscale Res. Lett.* **2009**, *4*, 1530–1539.
- [16] a) S.-H. Wang, C.-W. Lee, A. Chiou, P.-K. Wei, *J. Nanobiotechnol.* **2010**, *8*, 33; b) L. W. Zang, N. A. Monteiro-Riviere, *Toxicol. Sci.* **2009**, *110*, 138–155.

Received: October 26, 2011
Revised: December 12, 2011
Published online: